Journal of Physics:
Conference Series

PURPOSE-LED
PUBLISHING™

PAPER • **OPEN ACCESS**

Capacitance voltage curve simulations for different passivation parameters of dielectric layers on silicon

To cite this article: M A Sevillano-Bendezú *et al* 2020 *J. Phys.: Conf. Ser.* **1433** 012007

View the article online for updates and enhancements.

You may also like

- Physical criteria for the interface passivation layer in hydrogenated amorphous/crystalline silicon heterojunction solar cell
Lei Zhao, Guanghong Wang, Hongwei Diao et al.
- Visualization of traps at SiO_2/SiC interfaces near the conduction band by local deep level transient spectroscopy at low temperatures
Takayuki Abe, Yuji Yamagishi and Yasuo Cho
- Effect of GeO_2 deposition temperature in atomic layer deposition on electrical properties of Ge gate stack
Masayuki Kanematsu, Shigehisa Shibayama, Mitsuo Sakashita et al.

This content was downloaded from IP address 45.231.80.27 on 26/03/2026 at 15:09

Capacitance voltage curve simulations for different passivation parameters of dielectric layers on silicon

M A Sevillano-Bendezú[1], J A Dulanto[1], L A Conde[1], R Grieseler[1,2], J A Guerra[1] and J A Töfflinger[1]*

[1] Departamento de Ciencias, Sección de Física, Pontificia Universidad Católica del Perú, Av. Universitaria 1801, Lima 32, Peru

[2] Chair Materials for Electronics, Institute for Micro- and Nanotechnologies MacroNano®, Technische Universität Ilmenau, Gustav-Kirchhoff-Str. 7, 98693 Ilmenau, Germany

*E-mail: japalominot@pucp.edu.pe

Abstract. Surface passivation is a widely used technique to reduce the recombination losses at the semiconductor surface. The passivating layer performance can be mainly characterized by two parameters: The fixed charge density (Q_{ox}) and the interface trap density (D_{it}) which can be extracted from Capacitance-Voltage measurements (CV). In this paper, simulations of High-Frequency Capacitance-Voltage (HF-CV) curves were developed using simulated passivation parameters in order to examine the reliability of measured results. The D_{it} was modelled by two different sets of functions: First, the sum of Gaussian functions representing different dangling bond types and exponential tails for strained bonds. Second, a simpler U-shape model represented by the sum of exponential tails and a constant value function was employed. These simulations were validated using experimental measurements of a reference sample based on silicon dioxide on crystalline silicon (SiO_2/c-Si). Additionally, a fitting process of HF-CV curves was proposed using the simple U-shape D_{it} model. A relative error of less than 0.4% was found comparing the average values between the approximated and the experimentally extracted D_{it}'s. The constant function of the approximated D_{it} represents an average of the experimentally extracted D_{it} for values around the midgap energy where the recombination efficiency is highest.

1. Introduction

Surface passivation is used to prevent or reduce the recombination of charge carriers via defect states related to dangling bonds at the semiconductor surface [1]. Using an insulator layer as a passivating layer on the semiconductor surface, two types of mechanisms are defined whereby surface passivation acts.

On the one hand, there is the chemical passivation which is related to the reduction of the interface trap density (D_{it}) by decreasing the surface defect states through chemical bonding with the passivation material. On the other hand, the field effect passivation is quantified by the fixed charge density (Q_{ox}) inside the insulator layer and near the insulator/semiconductor interface. These fixed charges repel one type of charge carriers from the surface in order to reduce the recombination of remaining trapped

Content from this work may be used under the terms of the Creative Commons Attribution 3.0 licence. Any further distribution of this work must maintain attribution to the author(s) and the title of the work, journal citation and DOI.
Published under licence by IOP Publishing Ltd

charges of the other type [2]. These two passivation parameters (Q_{ox} and D_{it}) can be obtained through High-Frequency Capacitance-Voltage (HF-CV) measurements [3]. The presence of fixed charges in the passivating layer causes a net shift along the voltage axis in the HF-CV curve, whereas the D_{it} causes a change in the curve's slope. Thus, comparing the ideal curve ($Q_{\mathrm{ox}} = 0$ and $D_{\mathrm{it}} = 0$) with the experimentally measured one allows the extraction of both parameters assuming that these two effects are the only ones present [4]. Additional effects, such as insulator charge instabilities and charge injection from the semiconductor or contact side [5], as well as leakage currents [6], are often relatively hard to identify and, if not taken into consideration, may considerably alter the resulting passivation parameters obtained from the experimental HF-CV curves. Therefore, simulations of HF-CV curves offer the possibility to perform a deeper analysis of the passivating layers. Despite the availability of many tools [7], most of them only consider a single D_{it}-value in the midgap of the semiconductor bandgap at the interface. This paper presents two methods that introduce a wider range of the D_{it}-spectrum into the simulations of the HF-CV curves.

2. Experimental and simulations

2.1. The capacitance voltage curve

A MOS (Metal-Oxide-Semiconductor) system based on thermally grown amorphous silicon dioxide on crystalline silicon (a-SiO_2/c-Si) with (100) orientation was taken as a reference due to its charge stability and excellent passivation properties that have been widely studied [8]. A scheme of the MOS system is depicted in Figure 1(a). The native, thin SiO_x layer formed at the a-SiO_2/c-Si interface is crucial for the silicon surface passivation.

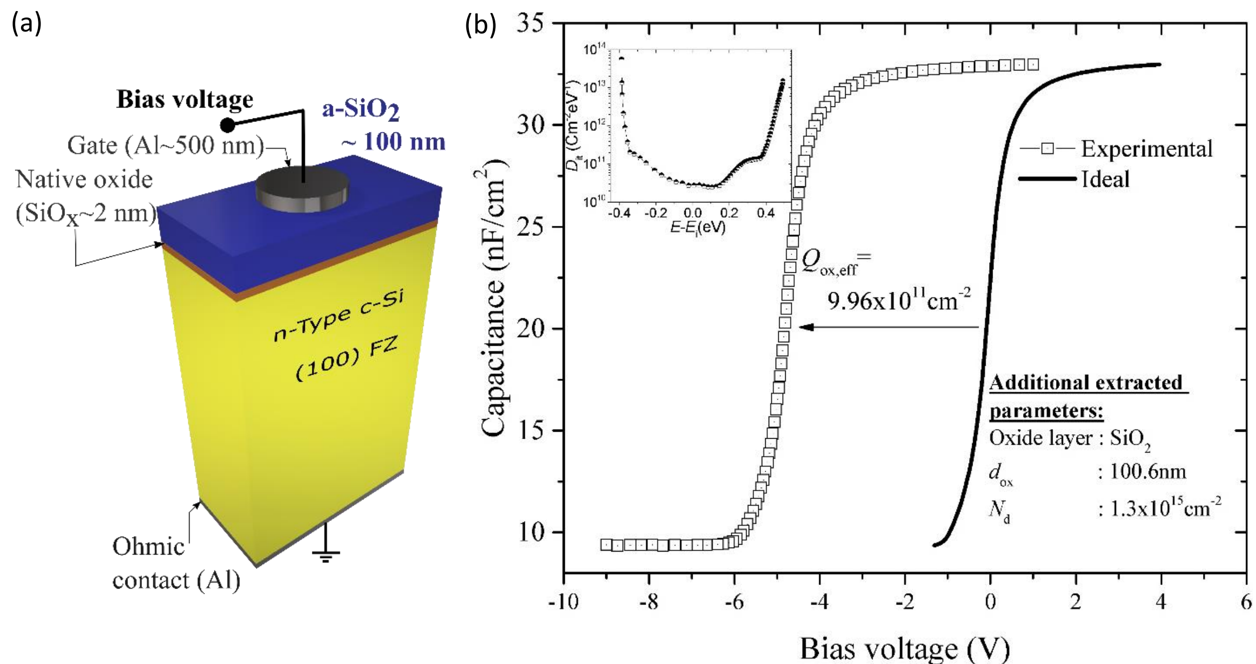

Figure 1. (a) MOS system scheme which represents the tested device used in order to obtain the HF-CV curves. A native oxide layer of SiO_x usually is formed at the SiO_2/c-Si interface. (b) Experimental and theoretical HF-CV curves are depicted. A shift is noticed due to the Q_{ox}. The experimentally extracted D_{it} over energy is shown in the inside diagram.

The experimentally measured HF-CV curve of this MOS system along with the corresponding calculated ideal curve is depicted in Figure 1(b). The experimental curve allows to obtain the oxide thickness (d_{ox}) = 100.6 nm and the semiconductor doping concentration (N_{d}) = 1.3×10^{15} cm^{-2}.

Furthermore, the comparison of these experimental and ideal HF-CV curves allows the extraction of the passivation parameters $Q_{\mathrm{ox}} = 9.96 \times 10^{11}$ cm^{-2} and D_{it} within the silicon bandgap energy with reference to the valence band energy. The latter is depicted in the inserted graph in Fig. 1(b). A detailed description of the method to extract these passivation parameters from the HF-CV curves can be found in [9,10,11].

2.2. Models for the D_{it} simulation

In this part of the paper we focus on the reverse procedure: the calculation and simulation of the HF-CV curves based on the modeling of the prior experimentally extracted passivation parameters from the reference MOS sample. Thenceforth, the D_{it} was simulated by means of two models in which the impact of the interface defect states originating from dangling bonds is taken as a variable added to the tail states originating from the strained bonds at the SiO_2/c-Si interface.

The first model is the one most accepted in the scientific community which considers electrically active amphoteric defect centers related to the SiO_2/c-Si interface [12,13]. Based on this model, the D_{it} at the (100) silicon surface is described mainly by P_{b0} and P_{b1}-type defect centers which in turn can be represented by Gaussian functions with two levels:

$$P_{\mathrm{b0}}^{\mathrm{Low,High}}(\epsilon_{\mathrm{t}}) = \frac{N_{\mathrm{t}}^{P_{\mathrm{b0,Low,High}}}}{w_{\mathrm{Low,High}}\sqrt{\frac{\pi}{2}}} e^{-2\frac{(E_{0;\mathrm{Low,High}}-\epsilon_{\mathrm{t}})^2}{w_{\mathrm{Low,High}}^2}} \quad (1)$$

$$P_{\mathrm{b1}}(\epsilon_{\mathrm{t}}) = \frac{N_{\mathrm{t}}^{P_{\mathrm{b1}}}}{w_1\sqrt{\frac{\pi}{2}}} e^{-2\frac{(E_1-\epsilon_{\mathrm{t}})^2}{w_1^2}} \quad (2)$$

Here, $P_{\mathrm{b0}}^{\mathrm{Low}}$ represents the Gaussian function associated to the P_{b0} defects centers with an energetic level in the lower part of the bandgap between the valence band and the midgap, whereas $P_{\mathrm{b0}}^{\mathrm{High}}$ levels are located between the midgap and the conduction band. P_{b1} is located very close to the midgap and can be represented by a single Gaussian function because its two levels are energetically indistinguishable.

Strained bonds at the bandgap edges are represented by exponential functions:

$$U_{\mathrm{T;v,c}}(\epsilon_t) = N_{\mathrm{v,c}} e^{-\beta_{\mathrm{v,c}}|E_{\mathrm{v,c}}-\epsilon_{\mathrm{t}}|} \quad (3)$$

Here, $U_{\mathrm{T;v}}$ is close to the valence band and $U_{\mathrm{T;c}}$ to the conduction band.

These functions depend on the trap level energy ϵ_{t} and the associated parameters in total are: $N_{\mathrm{t}}^{P_{\mathrm{b0,Low,High}}}$, $E_{0;\mathrm{Low,High}}$, $w_{\mathrm{Low,High}}$, $N_{\mathrm{t}}^{P_{\mathrm{b1}}}$, E_1, $N_{\mathrm{v,c}}$, β and $E_{\mathrm{v,c}}$, (altogether, 13 parameters) some of them are reduced by experimental facts as shown in [9].

Then, D_{it} is modelled by the sum of these functions:

$$D_{\mathrm{it}} = U_{\mathrm{T,v}} + P_{\mathrm{b0}}^{\mathrm{Low}} + P_{\mathrm{b1}} + P_{\mathrm{b0}}^{\mathrm{High}} + U_{\mathrm{T,c}} \quad (4)$$

The second model simplifies que prior model by considering a uniform, constant value for the interface defect state density D_{it}^0 along with the exponential tails used in the first part. Thus, equation (4) is reduced as follows:

$$D_{\mathrm{it}} = U_{\mathrm{T,v}} + D_{\mathrm{it}}^0 + U_{\mathrm{T,c}} \quad (5).$$

Subsequently a fit of the experimental HF-CV curve using the Gaussian D_{it} model and simplified constant D_{it} was performed.

3. Results and discussion

3.1. Evaluation of simulated HF-CV curves by applying simulated passivation parameters

As a first step, D_{it} has been simulated using the presented model based on Gaussians. The model to best fit the experimentally extracted data used the following parameters, summarized in Table 1.

Table 1. D_{it} simulation parameters

Dangling bond	$N_t^{P_{\text{b0,Low}}}$, $N_t^{P_{\text{b1}}}$, $N_t^{P_{\text{b0,High}}}$ (cm^{-2})	w_{Low}, w_{High}, w_1 (eV)	$E_{0,\text{Low}}$, E_1, $E_{0,\text{High}}$ (eV)
$P_{\text{b0}}^{\text{Low}}$	4.7×10^{10}	0.24	−0.375
P_{b1}	1.0×10^{10}	0.27	−0.010
$P_{\text{b0}}^{\text{High}}$	2.5×10^{10}	0.16	0.325
Strained bond	N_v, N_c (cm^{-2})	β_v, β_c (eV^{-1})	E_{v}, E_{c} (eV)
$U_{\text{T,v}}$	7.0×10^{15}	46	−0.56
$U_{\text{T,c}}$	2.6×10^{14}	46	0.56

The experimentally extracted as well as the simulated D_{it} and the associated functions are depicted in figure 2. The extreme points closest to the band edges were not fitted since the values around the midgap are more significant for recombination.

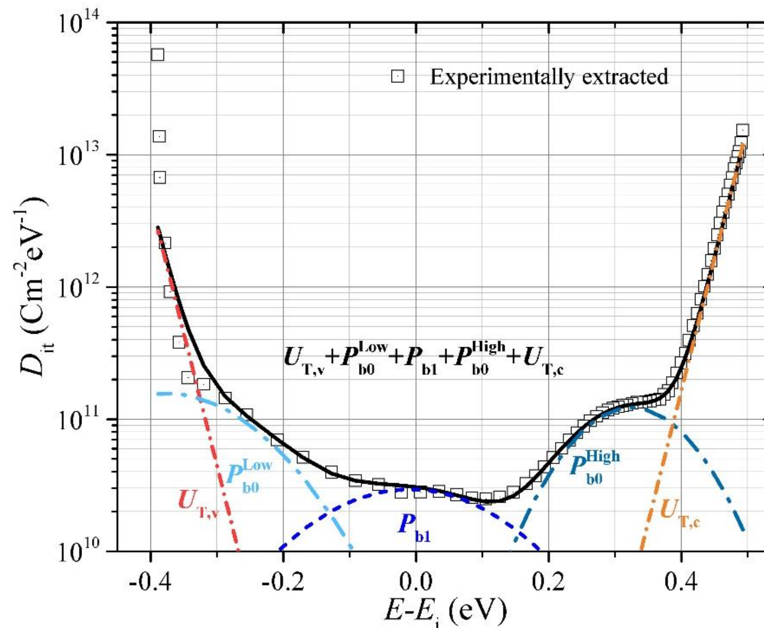

Figure 2. Comparison of the experimentally extracted and simulated D_{it} as the sum of the Gaussian distributions for defect centers P_{b0} and P_{b1} and exponentials U_{T} for the tail states.

The resulting HF-CV curve based on the simulated D_{it} is depicted in Figure 3(a) together with the experimental HF-CV data and a simulated curve resulting from $D_{\text{it}} = 0$. For simplicity, the degeneracy factor of $g = 1$ is assumed for the occupancy functions of donors as well as acceptors [8]. By comparing the simulated curves to the experimental data, the relative error is calculated and depicted in Fig. 3(b). On the one hand, the maximum relative error for the HF-CV curve without D_{it} is around 8% around the

flatband voltage (FB) and the minimum error is found around the midgap voltage. On the other hand, the HF-CV curve simulated using the modelled D_{it} presents a relative error far below 1% at any voltage.

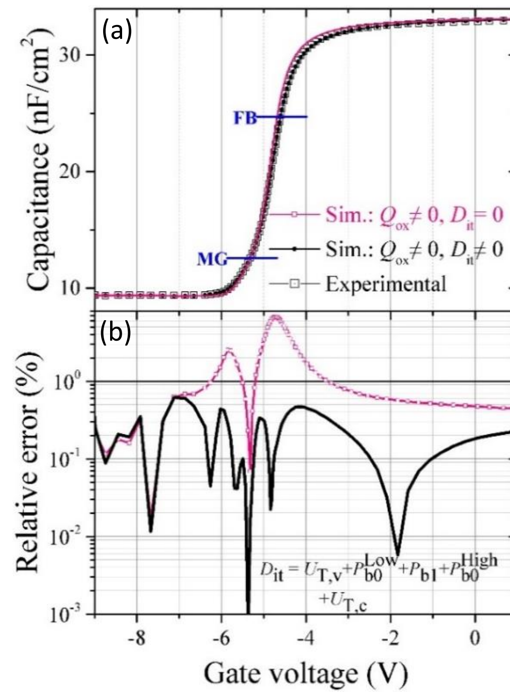

Figure 3. (a) Measured CV curve compared to simulated CV curve with D_{it} and without D_{it} are shown. The flatband (FB) and the midgap (MG) values are indicated. (b) Relative error associated to the simulated and measured HF-CV curves for $D_{\mathrm{it}} = 0$ and for the simulated D_{it} with Gaussian distributions for the defect centers P_{b0} and P_{b1}.

3.2. HF-CV curve fitting based on a simple U-shape D_{it} model through HF-CV curve simulations

The previous results were obtained using a simulated D_{it} based on the Gaussian and exponential functions model which required a relatively large amount of computational power due to the large number of parameters. In order to approximate the D_{it} in a less intricate way and with less computing time, the Gaussian functions were replaced by a constant value for D_{it} as shown already in Equation (5). With this model, the fitting parameters could be reduced to only three: The slope of the exponential functions (N_c and N_v) and the parameter D_{it}^0. Once appropriated ranges for these parameters were selected, three duplets of these parameters are taken into account to compare the mean square error (MSE) of the resulting simulated HF-CV curve with the experimental one. Thus, for a number of M experimental capacitance-voltage points, a value $S_{i,j,k}$, was calculated which is directly proportional to the MSE relating the difference between the experimental capacitance at specific *m* point C_m^{exp} with a simulated capacitance C_m^{sim}, as can be seen in the following expression:

$$S_{i,j,k} = \sum_{m=1}^{M} \left(C_m^{exp} - C_m^{sim}\left(D_{it,i}^0, N_{c,j}, N_{v,k}\right) \right)^2 \quad (6)$$

Where the subscripts i, j and *k* represent a specific combination of the model parameters. The total number of points with the optimized curve with minimum MSE is depicted in Figure 4. The

corresponded simulated HF-CV curve with minimum MSE is shown in figure 5(a). In contrast to the previous Gaussian method, due to the lower computational resources required by this new approach, we assumed degeneracy factors of $g = \frac{1}{2}$ and $g = 2$ for donors and acceptors, respectively, as suggested in [8].

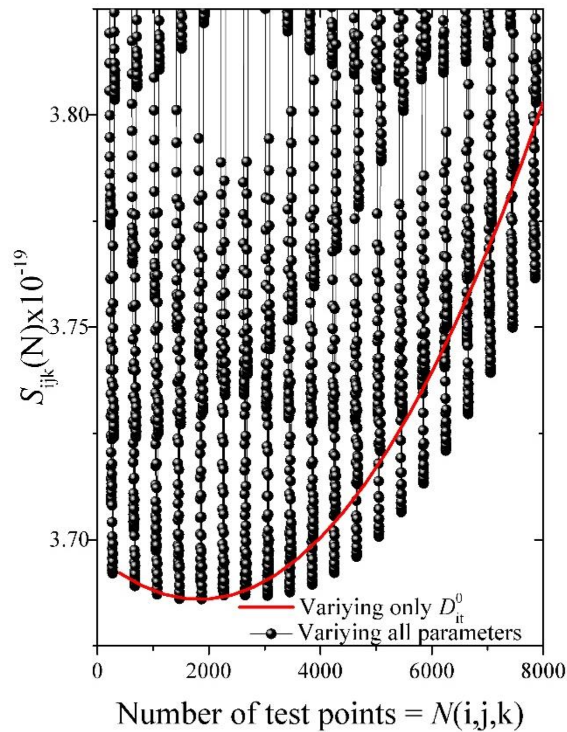

Figure 4. Each point represents a $S_{i,j,k}$ in selected ranges. In line red lies the point with minimum MSE.

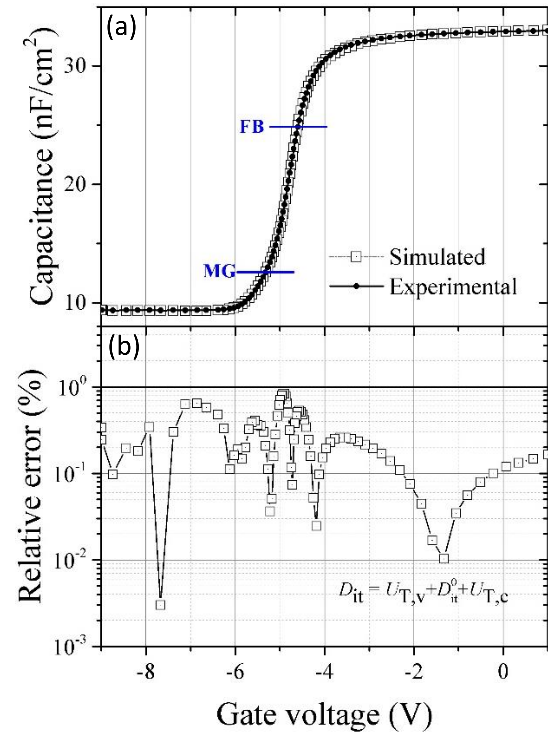

Figure 5. (a) Fitted and simulated HF-CV curves comparison. (b) The correspondent relative error less than of 1%.

The relative error depicted in Figure 5(b) is less than of 1% at any voltage when applying this simple U-shape model. Finally, the experimentally extracted and the approximated D_{it} are compared as shown in Figure 6. From this fitting procedure the following fitting parameters have been obtained: $D_{it}^0 = 4.54 \times 10^{10}$ cm^{-2}eV^{-1}, $N_c = 2.43 \times 10^{14}$ cm^{-2}eV^{-1} and $N_v = 1.52 \times 10^{15}$ cm^{-2}eV^{-1}.

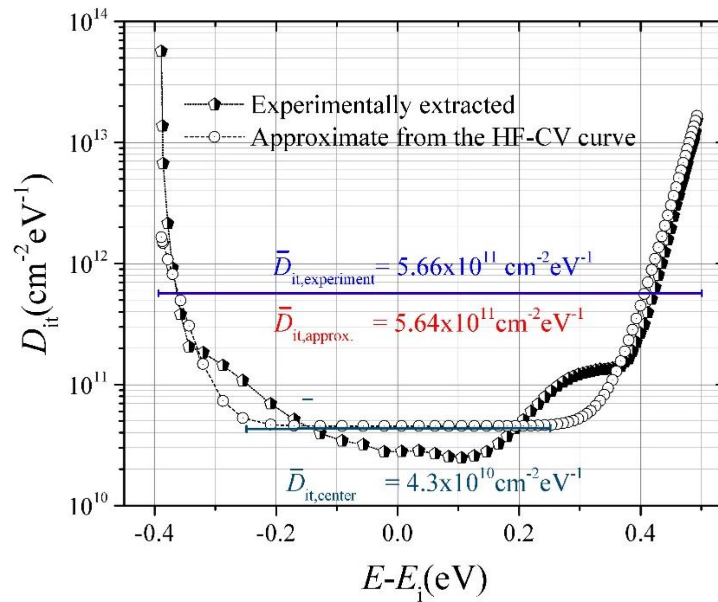

Figure 6. Comparison of the experimentally extracted and approximated D_{it} based on a simple U-shape model.

Additionally, the average of central values of the D_{it} around the midgap in the range between -0.25 eV to 0.25 eV ($\bar{D}_{\mathrm{it,center}}$) has been calculated, where most of the recombination processes occur [14]. Finally, a very good approximation is achieved when comparing the average D_{it} of the experimental data and the modeled data within the entire band gap. Here, a relative error of around 0.3 % indicates that this method allows to obtain an acceptable approximation of the $\bar{D}_{\mathrm{it}}$.

4. Conclusions

High-Frequency Capacitance-Voltage (HF-CV) curves were simulated for different passivation parameters at the SiO_2/c-Si interface using experimental data and different models to describe the interface defects states. A complex and a simplified method to simulate the HF-CV curves have been proposed based on different approximations of de D_{it} distribution: (1) Sum of Gaussians representing different defect centers and tail states represented by exponential functions, (2) Sum of a constant D_{it} value and the tail states. The second approach, which is computationally less complex results in a very good approximation of the experimental HF-CV curve. This was achieved by an algorithm that looks for the best fitting parameters that minimize the square error when comparing the experimental and the simulated curves. Both methods allow a reliable estimation of the passivation parameters and could be helpful to study other passivation materials that are not as stable or of similar high passivation quality as thermally grown SiO_2 on c-Si.

Acknowledgments

We thank Dr. Walter Füssel and Prof. César Guerra Gutierrez for the fruitful discussions. Support of the Peruvian National Council for Science, Technology and Innovation (CONCYTEC) is gratefully acknowledged: Contract N°132-2017. The authors are also thankful to the financial support given by FONDECYT through Contract N°045-2018. This research was also supported by the Research Managements Office (DGI) of the Pontificia Universidad Católica del Perú (PUCP) through grant no. CAP-2019-3-0041.

References

[1] Aberle A G, Glunz S, and Warta W 1992 *J. Appl. Phys.* 71 4422
[2] Bonilla R S, Hoex B, Hamer P and Wilshaw P R 2017 *Phys. Status Solidi A* 214 1700293
[3] Pierret R F 1996 *Semiconductor Device Fundamentals* (Addison Wesley)
[4] Terman L M 1962 *Solid State Electron* 5 285
[5] Yang B L, Lai P T and Wong H 2004 Microelectronics Reliability 44 70
[6] Yang K J and Chenming H 1999 IEEE Transactions on Electron Devices 46 1500
[7] Anwar S R M et al 2017 *IEEE Transactions on Electron Devices* 64 3786
[8] Nicollian E H and Brews J R 1982 *MOS (Metal Oxide Semiconductor) Physics and Technology* (Wiley Classics Library)
[9] Füssel W 1977 *Ermittlung und Analyse von Termspektren Si/SiO2-Phasengrenze als Beitrag zur Klaerung der Natur der Zustaende* (Berlin: PhD thesis)
[10] Henckel T 2011 *Intelligente Messwerterfassung der Hochfrequenz Kapazitätskennlinie* (Berlin: Bachelor Thesis)
[11] Töfflinger J A 2014 *Interface investigations of passivating oxides and functional materials on crystalline silicon* (Berlin: PhD thesis)
[12] Li P, Song Y, and Zuo X 2019 *Physica Status Solidi RRL* 13 1800547
[13] Flietner H 1995 *Materials Science Forum* 185-188 73
[14] Black L E 2016 *New Perspectives on Surface Passivation: Understanding the Si-Al2O3 Interface* (PhD thesis)